IEEE Photonics Journal
An IEEE Photonics Society Publication

Open Access

Fusion of Visible Light Indoor Positioning and Inertial Navigation Based on Particle Filter

Volume 9, Number 5, October 2017

Zhitian Li
Aiying Yang, *Member, IEEE*
Huichao Lv
Lihui Feng
Wenzhan Song

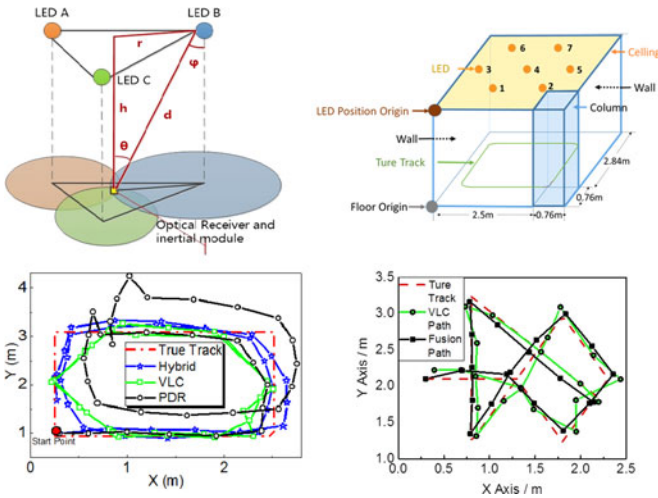

DOI: 10.1109/JPHOT.2017.2733556
1943-0655 © 2017 IEEE

IEEE photonics SOCIETY

IEEE

Fusion of Visible Light Indoor Positioning and Inertial Navigation Based on Particle Filter

Zhitian Li,[1] Aiying Yang,[1] *Member, IEEE*, Huichao Lv,[1] Lihui Feng,[1] and Wenzhan Song[2]

[1]School of Optoelectronics, Beijing Institute of Technology, Beijing 100081, China
[2]College of Engineering, University of Georgia, Athens, GA 30602 USA

DOI:10.1109/JPHOT.2017.2733556

Manuscript received July 8, 2017; revised July 25, 2017; accepted July 26, 2017. Date of publication July 31, 2017; date of current version September 19, 2017. This work was supported by the National Natural Science Foundation of China under Grants 61475094 and 61675025. Corresponding author: Aiying Yang and Lihui Feng (e-mail: yangaiying@bit.edu.cn; lihui.feng@bit.edu.cn).

Abstract: With the increasing demand for indoor positioning-based services, indoor positioning methods based on Bluetooth, Wi-Fi, ultra wide band (UWB), inertial navigation, and visual light communications (VLC) have been proposed. Considering the limitations of accuracy, cost and complexity, we propose a fusion positioning scheme integrating VLC positioning and inertial navigation base on particle filter. The experimental results demonstrated that the performance degradation caused by the multipath effect and light obstruction in VLC-based positioning and the cumulative error associated with inertial navigation are solved in the proposed fusion system. The accuracy of the fusion positioning system is in centimeters, which is two to four times better as compared to the VLC-based positioning or inertial navigation alone. Furthermore, the fusion positioning system has the advantages of high accuracy, energy saving, low cost, and easy to install, making it a promising candidate for future indoor positioning applications.

Index Terms: Indoor positioning, particle filter, inertial navigation, visible light communication based positioning.

1. Introduction

With the rapid advancement of smart equipment in recent years, location based service (LBS), i.e., employing different kinds of communication and positioning technologies to localize the walker and provide relevant services, start to develop immediately. Indoor positioning is still an open issue since the accuracy of satellite positioning severely degrades in the indoor environment. Nowadays, indoor positioning methods are mainly based on Wi-Fi, Bluetooth, RFID, visible light communications (VLC) and inertia navigation [1]–[5]. Comparison among these positioning method is shown as Table 1, and more comparison in detail can be found in Reference [4].

Compared with other positioning methods, indoor positioning based on visible light communication, so called VLC based positioning, has lots of unique advantages. VLC based positioning system can use existing LED lighting infrastructure with simple modifications, in other words, the system consider both positioning and lighting, thus it will save energy and realize high accuracy positioning with low cost at the same time [4]. Besides that, owing to the advantage of electromagnetic free, VLC based positioning is a green positioning method. Because of these advantages

TABLE 1
Comparison Among Different Indoor Positioning Method

	Accuracy	Anti-interference	Complexity	Cost
Wi-Fi	0.5 m–2.2 m	Great	Medium	Low
iBeacon	3 m–5 m	Medium	Medium	Medium
RFID	0.53 m–0.97 m	Great	Medium	Low
VLC	0.01 m–0.35 m	Weak	Low	Low

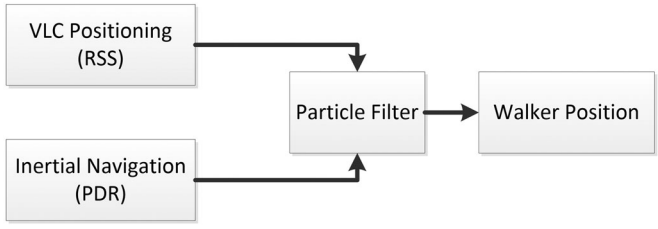

Fig. 1. Scheme setup of fusion indoor positioning scheme with inertial navigation and VLC based positioning.

we mentioned, VLC based positioning is seen as a promising candidate technology. However, two main shortcomings of the VLC based positioning, i.e., positioning failure due to the obstruction of visible light and accuracy degradation due to the multipath reflection effect [20], should be overcome before it comes into applications. Inertial navigation is an important positioning technique because it works automatically, and has the benefit of high short-term accuracy and great anti-interference ability. However, inertial navigation has a drawback that it cannot provide long-term accurate positioning because of the cumulative error with time. In this work, we proposed a fusion positioning scheme fusing the VLC based indoor positioning and inertial navigation with the deployment of particle filter. With the particle filter algorithm, the data from VLC positioning and inertial navigation are cross-processed to improve the positioning accuracy and solve the problems bottle necking the VLC positioning and inertial navigation. The remainder of this paper is arranged as follows: Section 2 describes the principle of the proposed fusion positioning scheme and the algorithm of particle filter to cross-process the data from VLC positioning and inertial navigation. Section 3 demonstrates the experimental results of the fusion positioning system. Finally, conclusions are addressed in Section 4.

2. Fusion Indoor Positioning Scheme With Inertial Navigation and VLC Based Positioning

2.1 Principle of the Fusion Indoor Positioning Scheme With Inertial Navigation and VLC Based Positioning

Fig. 1 is the setup of fusion indoor positioning scheme with VLC based positioning and inertial navigation. As shown in Fig. 1, A particle filter processes the data from two sources which includes the VLC positioning and inertial positioning, to estimate the accurate position of a walker. The VLC positioning data, i.e. the walker indoor coarse position, is acquired in a LED lighting environment with commonly used trilateral RSS (Received Signal Strength) algorithm [12], [13]. As Fig. 2 depicts, the proposed system configuration model for a typical indoor environment contains several VLC

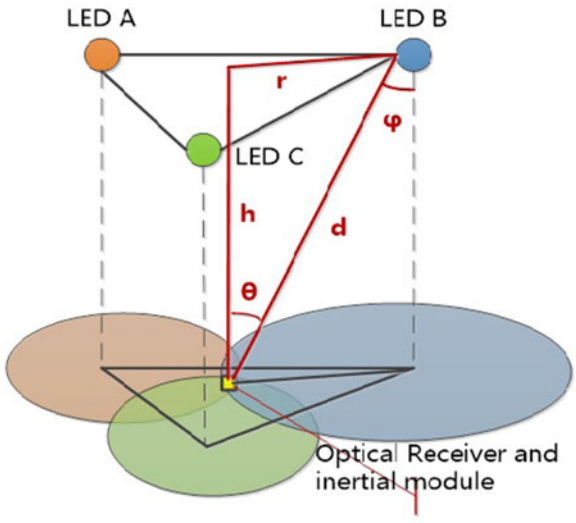

Fig. 2. The model of visible light positioning.

positioning units located on the ceiling, every unit has three LED bulbs which acts as a single optical transmitter. A unique code are assigned to every bulbs in order to ensure that the bulbs can be distinguished through their unique code. The LED bulbs are modulated into on-off keying (OOK) format. The receiver, including an optical detector and inertial module, is assumed to be a wearable mobile device. Based on the Lambert model, the channel gain of the LED bulb can be expressed as (1) [21]:

$$H(0) = \frac{(m+1)A\cos^m(\phi)\cos(\theta)}{2\pi d^2} \tag{1}$$

where A is the physical area of the photodiode detector in the VLC positioning module, θ is the angle of incidence with respect to the receiver axis, ϕ is the angle of incidence with respect to the LED bulb. m represents the order of Lambertian emission, and is denoted as (2):

$$m = \frac{-\ln 2}{\ln(\cos \Phi_{1/2})} \tag{2}$$

where $\Phi_{1/2}$ is the half power angle of the LED bulb. Generally, $\phi = \theta$, $m = 1$, $\cos\phi = h/d$, if we denote the light intensity of the LED bulbs transmitter and positioning module receiver as I_t and I_r respectively, we will achieve (3) as follows:

$$I_r = I_t \times H(0) = \frac{A}{\pi} \times \frac{I_t h^2}{d^4} = C \times \frac{I_t h^2}{d^4} \tag{3}$$

As shown in Fig. 2, we obtain (4) and (5) based on (3), which demonstrates the relationship among r, d, and h as follows:

$$r = \sqrt{d^2 - h^2} = (\sqrt{C \times h^2 \times I_t / I_r} - h^2)^{\frac{1}{2}} \tag{4}$$

$$(X - x)^2 + (Y - y)^2 = r^2 \tag{5}$$

where C is a constant. From (5), the position of the receiver can be obtained as (6):

$$\begin{cases} (X_A - x)^2 + (Y_A - y)^2 = r_A^2 \\ (X_B - x)^2 + (Y_B - y)^2 = r_B^2 \\ (X_C - x)^2 + (Y_C - y)^2 = r_C^2 \end{cases} \tag{6}$$

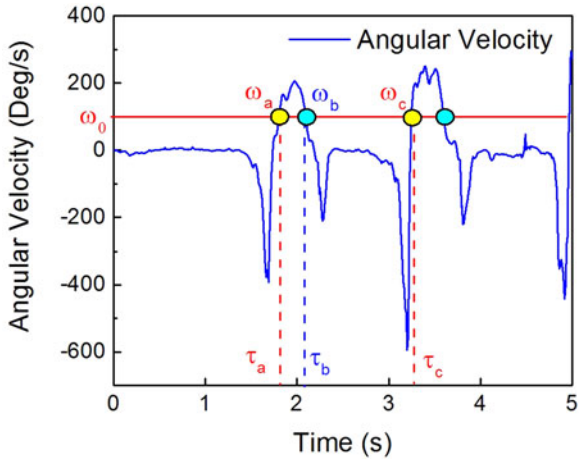

Fig. 3. Step count based on threshold detection of the heading angular velocity.

where (X_A, Y_A), (X_B, Y_B) and (X_C, Y_C) are the positions of LED A, LED B, and LED C; the terms r_A, r_B and r_C represent the distance from the LED A/B/C to the module; and (x, y) is the position of the module. So far we have get the VLC positioning data. To facilitate discussion, we regard the VLC position at time k as $Z[x_k, y_k]^T$.

The inertial navigation data which contains step frequency, heading direction and stride, are obtained by a pedestrian dead reckoning (PDR) module. PDR automates the self-positioning based on previous known position, the distance traveled and direction of travel. The classic PDR method has been reported in [6], [7]. In this work, a most popular foot-mounted PDR system is employed [8], [16]. In the PDR system, digital motion engine (DMP) of a MEMS module is used to obtain the real-time travel direction, and the distance traveled is obtained by step detection and stride estimation algorithm. Due to the step frequency of an adult is about 1-3 steps per second, we employ a 5Hz low pass filter to eliminate the high-frequency noise from the direction signal. The direction of travel at time k is denoted as θ_k. A method based on acceleration signal pattern has been proposed to detect step frequency in [9]. In the actual tests, we find that the heading angular velocity during walking is cyclic and has less high-frequency noise than the acceleration. So we count the step frequency by a method based on the threshold detection of heading angular velocity as shown in Fig. 3. We set an angular velocity threshold ω_0 and a time interval threshold τ_0. If the detected angular velocities ω_a and ω_b equaling to ω_0 are at neighboring time τ_a and τ_b respectively with $\tau_b - \tau_a < \tau_0$, the follow-up angular velocity detection will be continued till at the next time τ_c when the corresponding angular velocity $\omega_c = \omega_0$. If $\tau_c - \tau_a < \tau_0$ holds, a step will be counted. In Fig. 2, the counted step points are marked with yellow color and the discarded points are marked with blue color. There are two commonly used methods of stride estimation [10], [11], and we use Kim approach to estimate the stride for a general walker [6].

2.2 Fusion Algorithm of Particle Filter for Cross-Processing the Data From VLC Positioning and Inertial Navigation

Particle filter is a technique that implements a recursive Bayesian filter using the Sequential Monte-Carlo method. It is particularly good for dealing with non-linear and non-Gaussian estimation problems. It is based on a set of random samples with weights, called particles, for representing a probability density [18], [19]. Since Carpenter proposed the concept of particle filter, it becomes one of the most important methods to solve the nonlinear optimal estimation problem [14]. As an appropriate filter in non-linearity environment, particle filter has applied to visible light positioning such as the reference [13], [22], [23]. However, these existing researches in the field of visible light

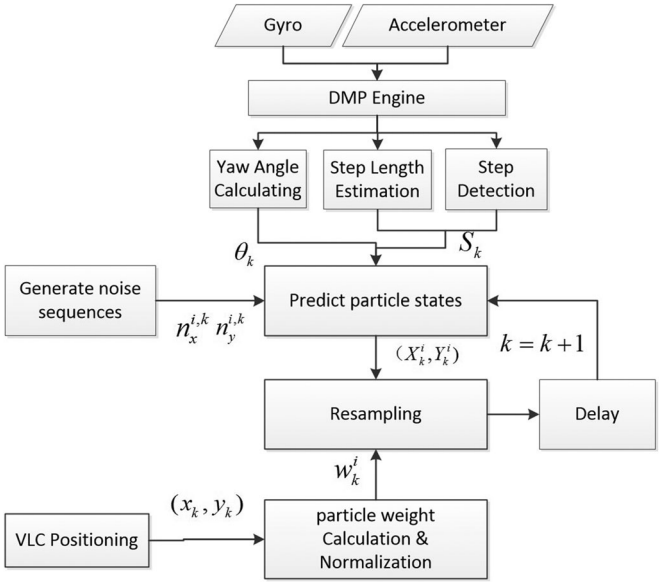

Fig. 4. Algorithm flowchart of fusion algorithm of particle filter.

positioning apply particle filter to eliminate the positioning results which are unreasonable with pure visible light positioning, and these method cannot mitigate the inherent problems of visible light positioning as we mentioned in Section 1. In order to solve the problems that inertial navigation has the cumulative error with time and visible light positioning has unexpected failure due to the obstruction of visible light and degraded accuracy due to multipath reflection effects, particle filter is used in Fig. 1 to cross-process the data from VLC positioning and inertial navigation. The fusion algorithm of particle filter is shown in Fig. 4, and a sequential importance resampling particle filter (SIR-PF) is implemented with the importance density and resampling performed in prior every time step as [17].

At the initialization step, a group of particles $\{\rho_1^i\}_{i=1}^{N_s}$ is generated on the basis of pre-established probability distribution $\{P(\rho_1^i)\}$, where N_s is the number of particles, ρ_1^i is the ith particle, and the weight of each particle is set to $1/Ns$. At time$k$, the state vector of the ith particle is (X_k^i, Y_k^i), where (X_k^i) and (Y_k^i) are the x-coordinate and y-coordinate respectively. With the kth stride, the particle group is updated from $\{\rho_k^i\}_{i=1}^{N_s}$ to $\{\rho_{k+1}^i\}_{i=1}^{N_s}$, the state of the ith particle is transited from (X_k^i, Y_k^i) to (X_{k+1}^i, Y_{k+1}^i) with the traveled distance S_k and direction angle θ_k obtained from the PDR module. The state transition of the ith particle is governed by the inertial navigation method and data as we mentioned in Section 2.1:

$$\begin{bmatrix} X_{k+1}^i \\ Y_{k+1}^i \end{bmatrix} = \begin{bmatrix} X_k^i \\ Y_k^i \end{bmatrix} + \begin{bmatrix} S_k \cos\theta_k \\ S_k \sin\theta_k \end{bmatrix} + \begin{bmatrix} n_k^{i,x} \\ n_k^{i,y} \end{bmatrix} \tag{7}$$

Considering the uncertainty associated with the inertial navigation, the state noise added to the ith particle is approximated by $(n_k^{i,x}, n_k^{i,y})$ on kth step. $n_k^{i,x}$ and $n_k^{i,y}$ are the state noise components of x-coordinate and y-coordinate which are zero mean white Gaussian process noise and generated by a random number generator [9].

Then, the weights of particles are calculated with the fusion of visible light positioning data as [15]

$$w_k^i = 1/\sqrt{2\pi R} \times exp(-(d_k^i)^2/2R) \tag{8}$$

where is the observation noise power with the consideration of uncertainty in the VLC positioning system, d_k^i is the distance between the coordinates of the ith particle and the VLC position at time$k$

and expressed by

$$d_k^i = \sqrt{(X_k^i - x_k^i)^2 - (Y_k^i - y_k^i)^2} \tag{9}$$

w_k^{*i} is then normalized to get the importance function by

$$w_k^{*i} = w_k^i / \sum_{i=1}^{N_s} w_k^i \tag{10}$$

Eqs. (8) and (10) indicate that the particles closer to the VLC positioning point have higher weights. The resampling step is critical in the process of particle filtering, because the variance of the particle weights quickly increases if the particle filter has no resampling step, which means very few normalized weights are substantial. Then, the inference is degraded because it is made by using only a very small number of particles. The idea of resampling is to remove the particle trajectories with small weights and replicate the trajectories with large weights [24]. In order to solve the degeneracy problem that only a few of the particles have significant weights, a resampling process is described in the following algorithm and carried as shown in Fig. 5.

Algorithm 1: Resampling Algorithm.

Input: Particles at time$k$, $\{\rho_k^i\}_{i=1}^{N_s}$;
Output: Particles after resampling at time k, $\{\rho_k^{*i}\}_{i=1}^{N_s}$;

```
i ← 1;
Calculate max weight among all the particle weights : max(w);
for i = 1 to N_s do
    // Generate a random number between 0 and 1: r and;
    // Set a weight limit:w_th = 2 × max(w) × r and ;
    // Generate a random integer between 1 and N_s:index;
    while w_th > w_index do
        // w_th ← w_th − w_index;
        // index ← index + 1;
        if index > N_s then
            // index ← 1;
        end if
    end while
    // ρ*^i_k = ρ^index_k;
    // i ← i + 1;
end for
```

When the resampling is completed, the obtained particles with the fusion of inertial navigation and visible light positioning data approach the actual position of the walker. The average position of all the particles (x_k^*, y_k^*) at time$k$ is regarded as the localization result of the hybrid positioning system.

3. Experimental Results

3.1 Structure of the Fusion Positioning System Integrating Inertial Navigation and VLC Based Positioning

Fig. 6 shows the structure of the fusion positioning system we demonstrated in the experiment. Considering that the altitude of VLC positioning module will affect the positioning performance, the VLC-based positioning module and the inertial navigation module we designed are individual modules, respectively, the walker can wear the VLC positioning module on the hand, shoulder, or head, among others, so the walker can hold the attitude of VLC positioning module easily. VLC

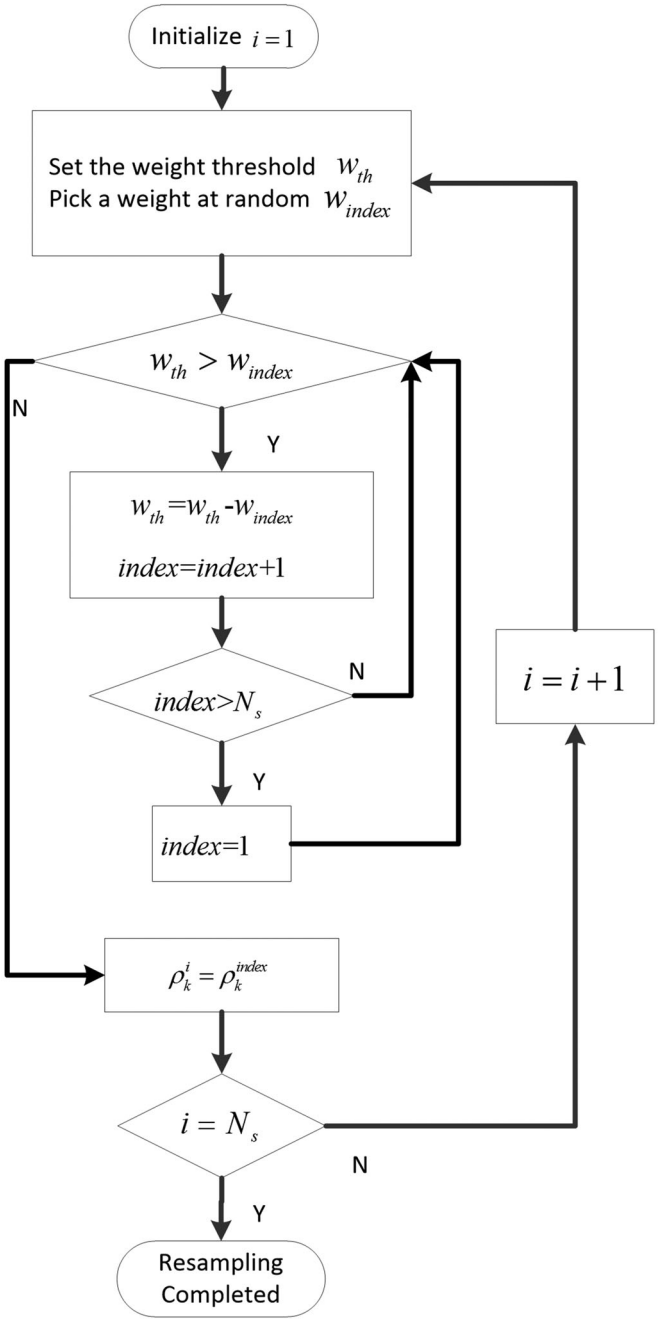

Fig. 5. Algorithm flowchart of particle resempling.

based positioning module and inertial navigation module sends the positioning data to the host computer respectively. In order to provide a portable and wearable positioning system, we use Bluetooth to connect VLC based positioning module and the host computer in our experiment, the inertial navigation module connect the host computer via serial port. In the host computer, the fusion algorithm based on particle filter iteratively runs to estimate the walker position. Fig. 7 is the hardware collecting and processing the VLC positioning data, which was wore with the walker. Fig. 8 is the hardware of MPU6050 MEMS module which is tied on the walkers tiptoe and collected the

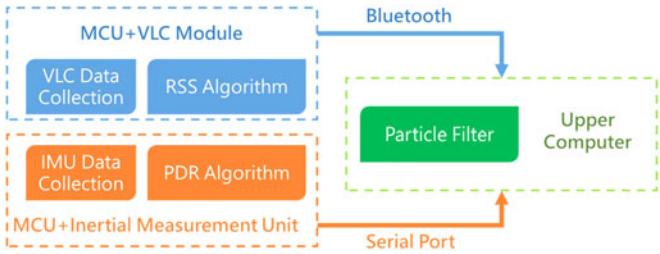

Fig. 6. Structure of the fusion positioning system integrating inertial navigation and VLC based positioning.

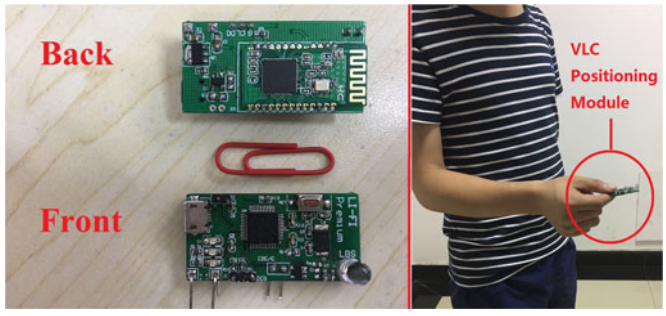

Fig. 7. Hardware of collecting and processing the visible light positioning data.

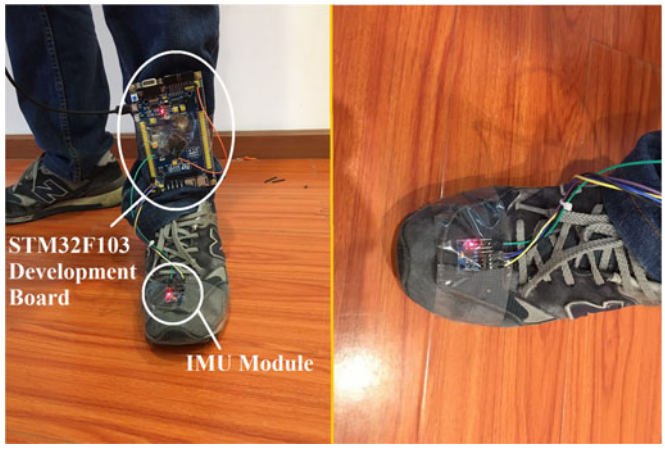

Fig. 8. Hardware of inertial navigation module.

original inertial movement data of the tiptoe. The inertial movement data is sent to a STM32F103 MCU (Microcontroller Unit) via I2C bus. Then, the MCU calculates the inertial navigation data and sends it to the host computer via serial bus.

3.2 Test Environment

Two test walks were conducted in the laboratory. As shown in Fig. 9(a), the experimental area of VLC positioning in a room is a hexagon with the side length of 1.5 m, where there are two sides close to the wall, and 2 corners and a column. Seven LED down lamps with the power of 17 W mounted on the ceiling serve as the lighting sources, and the ceiling height is 2.5 m. To set the

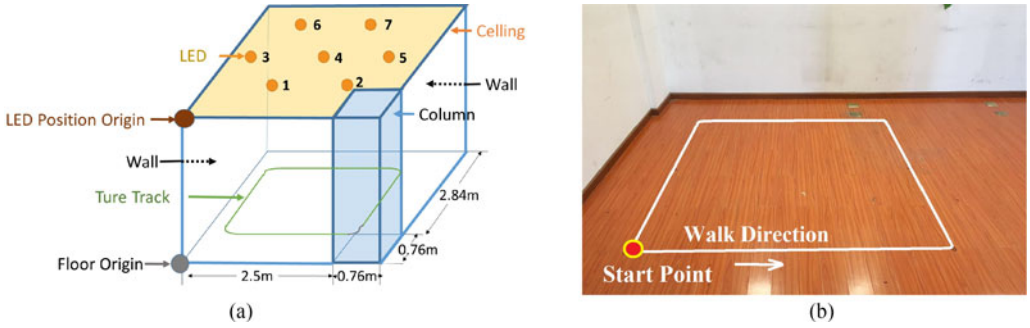

Fig. 9. Experiment Environment. (a) Experiment system layout with seven LED lamps as visible lighting sources. (b) the walking track of the tester.

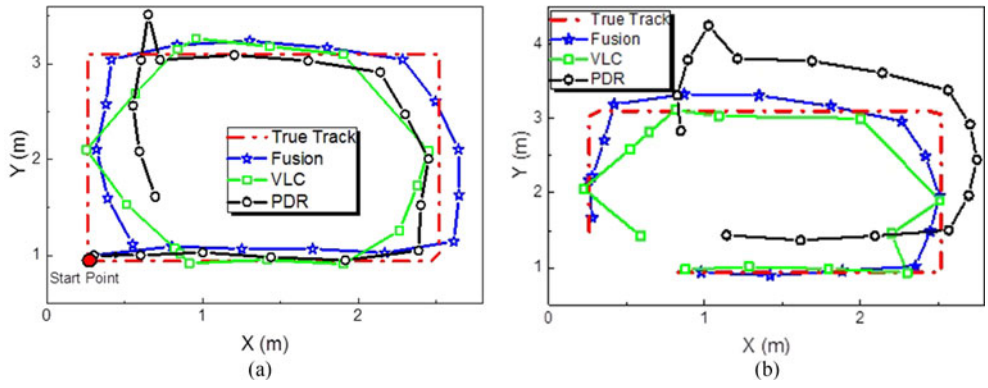

Fig. 10. Measured track with different positioning methods. (a) 1st walking lap. (b) 2nd walking lap.

origin at one corner of the room, the coordinates of seven LED sources in units of meter are (0.93, 0.888), (2.33, 0.888), (0.23, 2.1), (1.63, 2.1), (3.03, 2.1), (0.93, 3.312) and (2.33, 3.312). The first walking track is a square with 2.0 m side length as shown in Fig. 8(b). In order to mimic the longer track, the tester walked two cycles.

3.3 Experimental Results

Fig. 10 demonstrates the measured track by VLC positioning, inertial navigation (PDR) and the fusion positioning system. With VLC based positioning, the measured tracks in the 1st and 2nd laps are similar. The measured positions fluctuate around the column because of the multipath effect, and are limited by the LED projected hexagon area on the floor due to the weak light received around the corner. With inertial navigation, the positioning accuracy at the first 3/8 lap is high, but the positioning error increases in the following track. It is observed that, the measured track following the first 3/4 lap deviates far and far away from the true track. Fortunately, both the degradation of positioning accuracy around the corners and column in VLC positioning system and the cumulative error of the inertial navigation system are alleviated by the fusion positioning system. Figs. 11 and 12 shows the measured error and error cumulative distribution functions associated with different positioning methods respectively. The error properties of different positioning methods in this experiment are shown in Table 2. As shown in Table 2, the maximum error of VLC based positioning, inertial navigation and fusion position is 0.86 m, 1.47 m and 0.41 m respectively. The average error of VLC based positioning, inertial navigation and fusion positioning is 0.339, 0.520, and 0.144 meter respectively. It means that the positioning accuracy is improved by two and four times as compared with VLC positioning and inertial navigation respectively. Fig. 13(a) magnifies

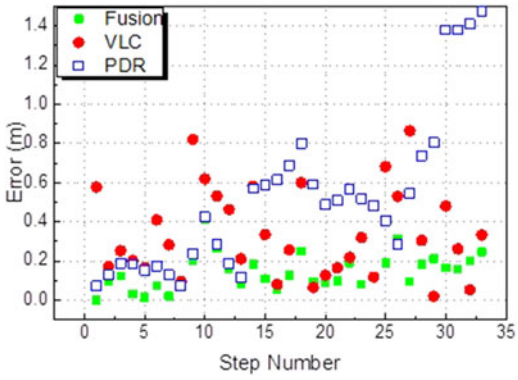

Fig. 11. Measured error with different positioning methods.

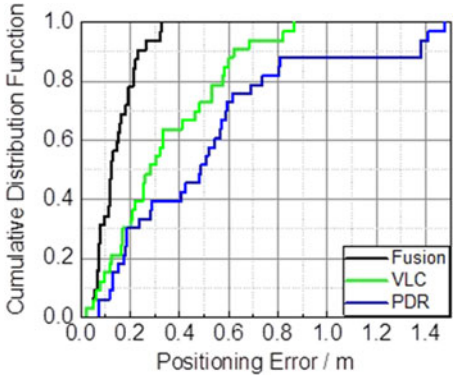

Fig. 12. Error cumulative distribution functions of VLC, PDR and fusion positioning.

TABLE 2
Positioning Error Comparison Among Different Positioning Algorithm in This Experiment

Error	VLC	INS	Fusion
Maximum	0.86 m	1.47 m	0.41 m
Average	0.339 m	0.52 m	0.14 m

the track around the column. It can be seen that the fusion positioning has better stability than visible light positioning. Fig. 13(b) and (c) compares the positioning error around the column. In the 1st lap, the step number that walker passed by the column is step 4–8. In the 2nd lap, the step number that walker passed by the column is step 21–24. The improvement of positioning accuracy obtained by fusion positioning becomes significant in the 2nd lap. Around the column, the average error of VLC positioning in two laps is 23 cm and 20 cm respectively, and is 4.5 cm and 12.13 cm of fusion positioning respectively. The positioning error is decreased by more than 50% with the fusion positioning.

Fig. 14(a) magnifies the track outside the projected hexagon area of 7 LEDs. The RSS based positioning algorithm requires that the light from at least three LEDs should be detected; otherwise

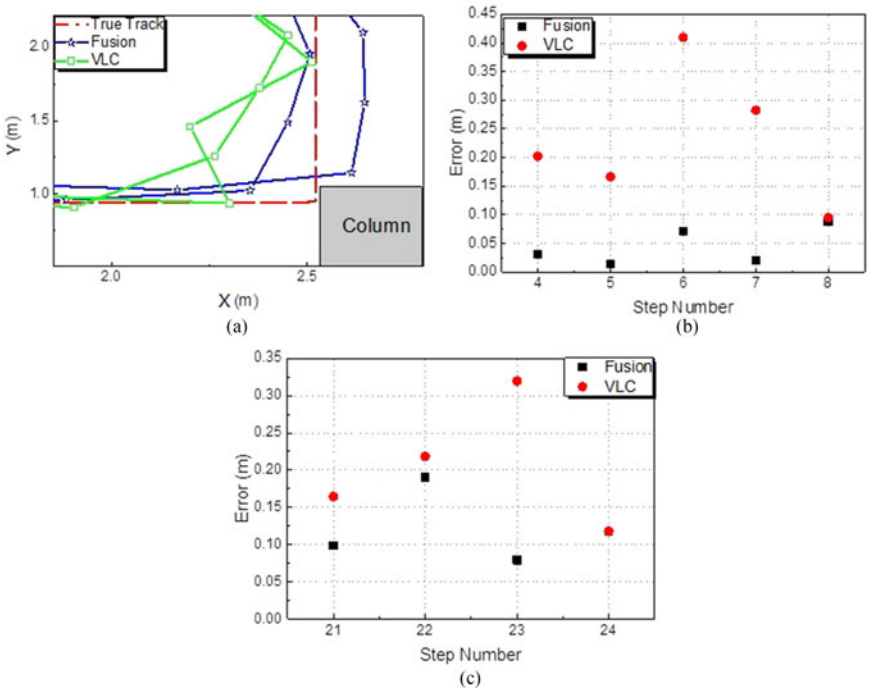

Fig. 13. Positioning performance around the column. (a) Magnified track around the column. (b) Positioning error around the column: Step 4–8 in the 1st lap. (c) Positioning error around the column: Step 21–24 in the 2nd lap.

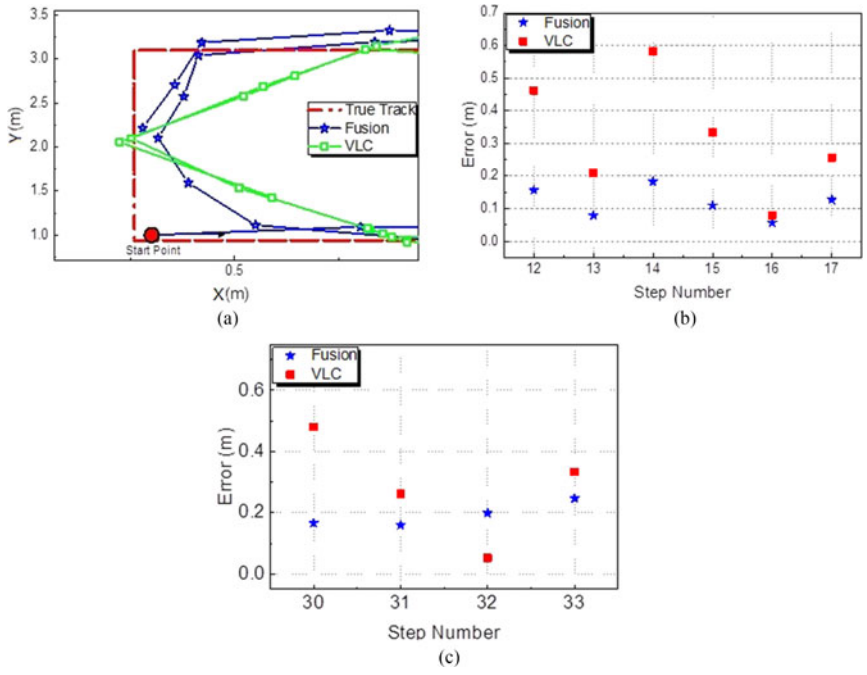

Fig. 14. Positioning performance outside the projected hexagon area of 7 LEDs. (a) Magnified outside the projected hexagon area of 7 LEDs (b) Positioning error outside the projected hexagon area of 7 LEDs: Step 12–17 in the 1st lap. (c) Positioning error outside the projected hexagon area of 7 LEDs: Step 30–33 in the 2nd lap.

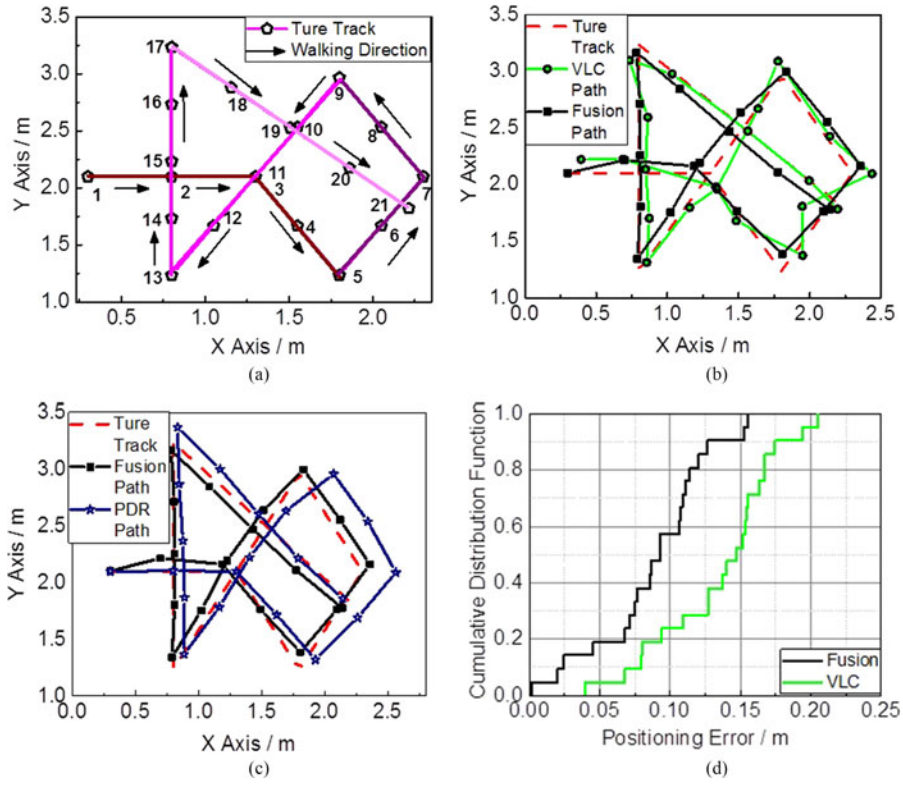

Fig. 15. Positioning performance in complex and extreme condition. (a) The true rtack of walking. (b) Fusion positioning and VLC positioning result in a complex trajectory. (c) Fusion positioning and PDR positioning result in a complex trajectory. (d) Error cumulative distribution functions of VLC and PDR positioning.

the VLC positioning cannot resolve the walkers position. As a result, the measured track by VLC positioning excludes the area outside the hexagon layout area. With the aid of inertial navigation, the fusion positioning can provide accurate position even outside the hexagon projection area. The positioning error around the corner is evaluated in Fig. 14(b) and (c). The fusion positioning error is much lower than the VLC positioning. The above experimental results indicate that, with the fusion positioning scheme based on particle filter, the problems of VLC positioning and inertial navigation can be solved. Both the positioning accuracy and stability are improved with comparison of VLC positioning and inertial navigation. In the experiment, the measurement is carried for a general walker with common walking behavior, thus the positioning performance will keep the same if the fusion positioning system is applied in practical scenarios with larger area.

In order to verify the positioning performance in complex and extreme condition, we also conducted another experiment with a more complicated track, and the entire track was inside the hexagon area made by the seven LEDs, which was designed with little VLC signal limited area to simulate true application scenarios. As Fig. 15 shows, the experiment result shows that the fusion positioning provides an improvement of 35.06% relative to VLC positioning regarding the mean error, which indicates that the fusion positioning system can also provide a better positioning result in a complex trajectory and condition.

4. Conclusion

In this work, we present a fusion positioning scheme fusing the VLC based indoor positioning and inertial navigation with the deployment of particle filter. With a sequential importance resampling

particle filter, the data from VLC based positioning and inertial navigation is cross-processed to obtain the accurate position of a walker. The experiments on a general walk demonstrate that, our proposed fusion positioning system addressed the problems encountered with the VLC based positioning and inertial navigation well, and the positioning accuracy and stability are improved. The maximum and average positioning error of fusion positioning system is 0.41 m and 0.14 m, which is 2 and 4 times better than VLC based positioning and inertial navigation alone respectively. It is worth mentioning that all the algorithm can be easily transplanted into other platform, and the foot-mounted hardware can also be replaced by hand-hold devices like smartphone and tablet with some algorithm adjustment, thus the fusing positioning system we proposed can be used in consumer-grade electronics, such as client guides in markets, museums, and indoor navigation systems in hospital, and it can also be used for industrial purposes, i.e., robots or AGV self-navigation, and the accuracy of fusion positioning system remains the same in practical scenarios of larger area.

References

[1] C. Yang and H. R. Shao, "WiFi-based indoor positioning," *IEEE Commun. Mag.*, vol. 53, no. 3, pp. 150–157, Mar. 2015.
[2] X. Y. Lin, T. W. Ho, C. C. Fang, Z. S. Yen, B. J. Yang, and F. Lai, "A mobile indoor positioning system based on iBeacon technology," in *Proc. Int. Conf. IEEE Eng. Med. Biol. Soc.*, 2015, pp. 4970–4973.
[3] C. H. Huang, L. H. Lee, C. C. Ho, L. L. Wu, and Z. H. Lai, "Real-time rfid indoor positioning system based on kalman-filter drift removal and heron-bilateration location estimation," *IEEE Trans. Instrum. Meas.*, vol. 64, no. 3, pp. 728–739, Mar. 2015.
[4] N. U. Hassan, A. Naeem, M. A. Pasha, T. Jadoon, and C. Yuen, "Indoor positioning using visible led lights: A survey," *ACM Comput. Surv.*, vol. 48, pp. 1–32, 2015.
[5] R. Harle, "A survey of indoor inertial positioning systems for pedestrians," *Commun. Surv. IEEE Commun. Surveys Tuts.*, vol. 15, no. 3, pp. 1281–1293, Jul.–Sep. 2013.
[6] J. W. Kim, J. J. Han, D. H. Hwang, and C. Park, "A step, stride and heading determination for the pedestrian navigation system," *Positioning*, vol. 3, pp. 273–279, 2004.
[7] T. Judd, "A personal dead reckoning module," *Proc. 10th Int. Tech. Meeting Satellite Division Inst. Navig.*, 1997, pp. 47–51.
[8] J. Elwell, "Inertial navigation for the urban warrior," *Proc. SPIE*, vol. 3709, pp. 196–204, 1999.
[9] H. Leppkoski, J. Collin, and J. Takala, "Pedestrian navigation based on inertial sensors, indoor map, and WLAN signals," *J. Signal Process. Syst.*, vol. 71, pp. 287–296, 2013.
[10] H. Weinberg, "Using the ADXL202 in pedometer and personal navigation applications," *Analog Devices AN-602 Application Note*, vol. 2, pp. 1–6, 2002.
[11] J. Scarlett, "Enhancing the performance of pedometers using a single accelerometer," Analog Devices AN-900 Application Note, 2007.
[12] Z. Zhou, M. Kavehrad, and P. Deng, "Indoor positioning algorithm using light-emitting diode visible light communications," *Opt. Eng.*, vol. 51, pp. 527–529, 2012.
[13] D. Ganti, W. Zhang, and M. Kavehrad, "VLC-based indoor positioning system with tracking capability using Kalman and particle filters," *IEEE Int. Conf. Consum. Electron.*, 2014, pp. 476–477.
[14] J. Carpenter, P. Clifford, and P. Fearnhead, "Improved particle filter for nonlinear problems," *IEE Proc. - Radar Sonar Navig.*, vol. 146, pp. 2–7, 1999.
[15] F. Evennou and F. Marx, "Advanced integration of WIFI and inertial navigation systems for indoor mobile positioning," *EURASIP J. Adv. Signal Process.*, vol. 2006, pp. 164–164, 2006.
[16] A. R. J. Ruiz, F. S. Granja, J. C. Prieto Honorato, and J. I. G. Rosas, "Accurate pedestrian indoor navigation by tightly coupling foot-mounted IMU and RFID measurements," *IEEE Trans. Instrum. Meas.*, vol. 61, no. 1, pp. 178–189, Jan. 2012.
[17] C. Gentner, E. Muoz, M. Khider, and E. Staudinger, "Particle filter based positioning with 3GPP-LTE in indoor environments," in *Proc. IEEE/ION Position Location Navig. Symp.*, 2012, pp. 301–308.
[18] F. Gustafsson *et al.*, "Particle filters for positioning, navigation, and tracking," *IEEE Trans. Signal Process.*, vol. 50, no. 2, pp. 425–437, Feb. 2002.
[19] Widyawan, M. Klepal, and S. Beauregard, "A backtracking particle filter for fusing building plans with PDR displacement estimates, navigation, and tracking," in *Proc. 5th Workshop Positioning, Navig. Commun.*, 2008, pp. 207–212.
[20] W. Gu, M. Aminikashani, P. Deng, and M. Kavehrad, "Impact of multipath reflections on the performance of indoor visible light positioning systems," *J. Lightw. Technol.*, vol. 34, no. 10, pp. 2578–2587, May 2015.
[21] T. Komine and M. Nakagawa, "Fundamental analysis for visible-light communication system using LED lights," *IEEE Trans. Consum. Electron*, vol. 50, no. 1, pp. 100–107, Feb. 2004.
[22] M. Jiang *et al.*, "Indoor anti-occlusion visible light positioning systems based on particle filtering," *Opt. Rev.*, vol. 22, no. 2, pp. 294–298, 2015.
[23] W. Gu, W. Zhang, J. Wang, M. R. A. Kashani, and M. Kavehrad, "Three dimensional indoor positioning based on visible light with Gaussian mixture sigma-point particle filter technique," *Proc. SPIE*, vol. 9387, Feb. 2015, Art. no. 93870O.
[24] M. Bolic, P. M. Djuric, and S. Hong, "Resampling algorithms and architectures for distributed particle filters," *IEEE Trans. Signal Process.*, vol. 53, no. 7, pp. 2442–2450, Jul. 2005.